Optimized control of Stark-shift-chirped rapid adiabatic passage in a Λ-type three-level system

Johann-Heinrich Schönfeldt,* Jason Twamley, and Stojan Rebić
Centre for Quantum Computer Technology, Physics Department, Macquarie University, Sydney, New South Wales 2109, Australia
(Received 6 May 2009; published 1 October 2009)

Inhomogeneous broadening of energy levels is one of the principal limiting factors for achieving "slow" or "stationary" light in solid-state media by means of electromagnetically induced transparency, a quantum version of stimulated Raman adiabatic passage (STIRAP). Stark-shift-chirped rapid adiabatic-passage (SCRAP) has been shown to be far less sensitive to inhomogeneous broadening than STIRAP, a population transfer technique to which it is closely related. We further optimize the pulses used in SCRAP to be even less sensitive to inhomogeneous broadening in a Λ-type three-level system. The optimized pulses perform at a higher fidelity than the standard Gaussian pulses for a wide range of detunings (i.e., large inhomogeneous broadening).

DOI: 10.1103/PhysRevA.80.043401 PACS number(s): 32.80.Qk, 33.20.Bx, 33.80.Be, 42.50.Hz

I. INTRODUCTION

Atomic vapors have been extensively investigated for use as quantum information storage media by "slowing down," or even "stopping," a light pulse carrying quantum information. This is achieved by mapping the quantum state of the light to a long-lived spin state in an ensemble of atoms by means of a reversible process: electromagnetically induced transparency (EIT) [1–5], which is closely related to an adiabatic passage technique known as stimulated Raman adiabatic passage (STIRAP) [6,7]. The homogeneity of the atomic vapor atoms means that the light pulses used in EIT experiments in these systems can be tuned to specific transitions in the atoms and that these light fields will then interact strongly with all the atoms in the ensemble.

Solid-state implementations of stored light by means of EIT may have a number of potential advantages over atomic vapor implementations. They have the potential to greatly reduce (possibly eliminate) limitations on the storage lifetime, which is mainly due to atomic diffusion and Doppler velocities in atomic vapor systems. A higher atomic density has the potential to yield a stronger interaction between the light and atomic ensemble, while being more compact and simple to use or manufacture may indicate great scalability [8] on the part of solid-state implementations. EIT and slow light have been demonstrated in rare-earth doped semiconductors, e.g., Pr-doped Y_2SiO_5 [9,10], whereas only EIT has thus far been shown in nitrogen-vacancy color centers in diamond [11,12]. Solid-state media are, however, not without their own problems, the biggest of which is inhomogeneous broadening of the energy levels, which leads to a reduction in the number of atoms or centers that will be resonant with the incident optical fields. This broadening occurs because each atom or center experiences a different electronic environment due to a number of factors, e.g., the local strains in the crystal lattice.

Recently a variation of STIRAP (the basis of EIT), namely Stark-shift-chirped rapid adiabatic passage (SCRAP), has been shown to perform coherent population transfer with a high fidelity for a range of different detunings in a Λ-type three-level system [13]. That is, SCRAP is far more robust when there is large inhomogeneous broadenings present in the ensemble. In SCRAP, a separate (pulsed) field is added to the STIRAP fields to induce Stark-shifts in the energy levels and thus bring the required, initially off-resonant, transitions on resonance at specific times. We propose that a quantum version of SCRAP could surmount some of the limitations that inhomogeneous broadening places on "slow" light in solid-state systems. We will examine this further in future work.

In this work we make use of optimum control techniques similar to Khaneja *et al.* [14], in order to optimise the standard SCRAP pulses so as to minimize the decrease in fidelity brought on by inhomogeneous broadenings of the transitions. To measure this we simulate the SCRAP process population transfer between two long-lived ground states which experience large detunings due to inhomogeneous broadening. Our main result is that we can improve the average fidelity of population transfer over a wide range of detunings for both the ground to excited state detuning and the ground to target state detuning (two-photon detuning). The optimal control pulses are thus tailored to provide effective state transfer (and thus EIT), in the presence of large inhomogeneous broadening.

The paper is arranged as follows: in Sec. II the SCRAP technique is introduced. Section III describes the optimization methods used. Section IV shows the results for the optimized pulses. Conclusions are drawn in Sec. V.

II. SCRAP

The SCRAP technique was first proposed by Yatsenko *et al.* [15], and implemented by Rickes *et al.* [16], in two-level systems as an efficient method for complete population transfer between two states. It was later shown by Rangelov *et al.* [13], that a Stark-shifting pulse can also be used to achieve complete population transfer through adiabatic passage in a three-level system, thus providing an alternative to STIRAP.

The Λ-type three-level system (Fig. 1), is comprised of two long-lived ground states, one the initially populated state ($|1\rangle$), and the other the target state ($|3\rangle$), and an excited state ($|2\rangle$). In general the excited state has a short life time:

*jhschonf@ics.mq.edu.au

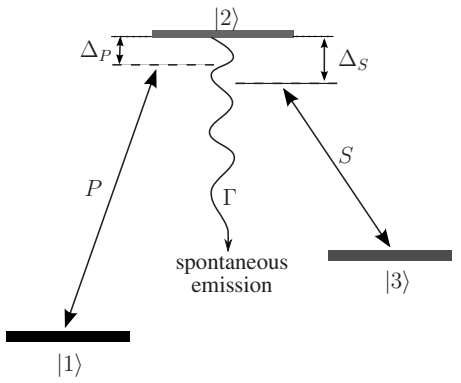

FIG. 1. The Λ-type three-level energy scheme. States $|1\rangle$ and $|2\rangle$ are coupled by the pump pulse P which has a detuning Δ_P from being exactly on resonance. Similarly states $|2\rangle$ and $|3\rangle$ are coupled by the Stokes pulse S which has a detuning Δ_S. State $|2\rangle$ is short lived with spontaneous emission occurring out of the system.

STIRAP is effective at complete population transfer since it avoids populating the excited state by having the system evolve along a dark-state. In both SCRAP and STIRAP states $|1\rangle$ and $|2\rangle$ are coupled by the "pump" laser pulse while states $|3\rangle$ and $|2\rangle$ are coupled by the "Stokes" laser pulse. The frequencies of these two classical laser fields are typically not exactly on resonance with their respective transitions, and have detunings Δ_P and Δ_S for the pump and Stokes lasers respectively. Herein lies the advantage that SCRAP has over STIRAP: STIRAP requires exact two-photon resonance ($\Delta_P-\Delta_S=0$) in order to be effective, whereas SCRAP has a larger tolerance for two-photon detuning. In SCRAP a third strong far-off-resonance laser pulse, the Stark pulse, is also applied. The Stark pulse induces a Stark-shift in the energy of the excited state (essentially leaving the energy of the lower levels unchanged), thus bringing the initially off-resonant transitions into resonance. The Stark-shift causes the diabatic energy of state $|2\rangle$ to cross those of states $|1\rangle$ and $|3\rangle$, allowing population transfer from $|1\rangle$ to $|2\rangle$ and then to $|3\rangle$, completing the population transfer. It is thus clear that the diabatic energies of state $|1\rangle$ and $|2\rangle$ must cross before the crossing of energies of states $|2\rangle$ and $|3\rangle$. It is also clear that decay out of the excited state will play a role in SCRAP, as opposed to STIRAP.

In the rotating wave approximation, the Hamiltonian of the Λ-type three-state system depicted in Fig. 1 is

$$H(t)=\frac{\hbar}{2}\begin{bmatrix}0 & \Omega_P(t) & 0\\ \Omega_P(t) & 2[\Delta_P+S_2(t)]-i\Gamma & \Omega_S(t)\\ 0 & \Omega_S(t) & 2(\Delta_P-\Delta_S)\end{bmatrix}, \quad (1)$$

where $\Omega_P(t)$ and $\Omega_S(t)$ are respectively the pump and Stokes laser field Rabi frequencies and $S_2(t)$ is the Stark-shift in the energy of the excited energy level $|2\rangle$ due to a third far-off-resonance laser pulse (Stark pulse). For the examples here it is assumed that the Stark-shift is negative, $S_2(t)<0$. The detunings of the pump and Stokes fields are Δ_P and Δ_S, respectively. The imaginary term $i\Gamma$ describes the losses from $|2\rangle$ due to spontaneous radiative decay out of the three-level system. Dephasing of state $|3\rangle$, is not included in this model since it is assumed that the pulse durations are much shorter than the decoherence times. This assumption is validated by noting that the decoherence time for NV centers, for example, is of the order of hundreds of microseconds [17]. The Stark-shifts of the energy levels for states $|1\rangle$ and $|3\rangle$ are not included here because Stark-shifts in ground and metastable states tend to be much smaller than those of excited states.

In Rangelov *et al.* [13], Gaussian pulse shapes were used for all the pulses, with identical peak values, Ω_0, for the Rabi frequencies of the pump and Stokes pulses,

$$\Omega_p(t)=\Omega_0 e^{-(t-\tau_p)^2/T_P^2}, \quad (2)$$

$$\Omega_s(t)=\Omega_0 e^{-(t-\tau_s)^2/T_S^2}, \quad (3)$$

$$-S_2(t)=S(t)=S_0 e^{-t^2/T_{St}^2}. \quad (4)$$

The peak of the Stark pulse (maximum Stark-shift of S_0) is taken to be at $t=0$, and as such the pump and Stokes pulses peak at times τ_p and τ_s, respectively. The pulse durations are determined by T_P, T_S, and T_{St}, where it was taken that the pump and Stokes pulses have equal duration $T_P=T_S$ and the Stark pulse has twice their duration $T_{St}=2T_P$. The unit of time was defined as T_P and the unit of frequency as $1/T_P$. These Gaussian pulses served as exemplars for the initial pulses used in our optimizing routine, see Sec. III.

The diabatic energies of the states are

$$E_{|1\rangle}=0, \quad (5)$$

$$E_{|2\rangle}=2[\Delta_P+S_2(t)], \quad (6)$$

$$E_{|3\rangle}=2(\Delta_P-\Delta_S), \quad (7)$$

which with the condition that the Stark-shift is negative $[S_2(t)<0]$, dictates that the diabatic energy of state $|2\rangle$, $E_{|2\rangle}$, will only cross those of states $|1\rangle$ and $|3\rangle$ when

$$S_0>\Delta_P>0, \quad (8)$$

and

$$S_0>\Delta_S>0. \quad (9)$$

With the condition that the Stark-shift is negative two distinct situations can arise: the two-photon detuning can be negative

$$\Delta_P>0>(\Delta_P-\Delta_S)>\Delta_P-S_0, \quad (10)$$

or positive

$$\Delta_P>(\Delta_P-\Delta_S)>0>\Delta_P-S_0. \quad (11)$$

In the examples used here to explain the SCRAP technique, and for the pulse optimization, only the first case Eq. (10), where the two-photon detuning is negative will be presented ($\Delta_P<\Delta_S$). In the case that the two-photon detuning is positive Eq. (11), the order of the pulses in standard SCRAP must be run in reverse to what will be shown here [13].

Our goal is to achieve efficient state transfer for as wide a variety of detunings as possible, for which SCRAP is the ideal technique. The population transfer for the ideal situa-

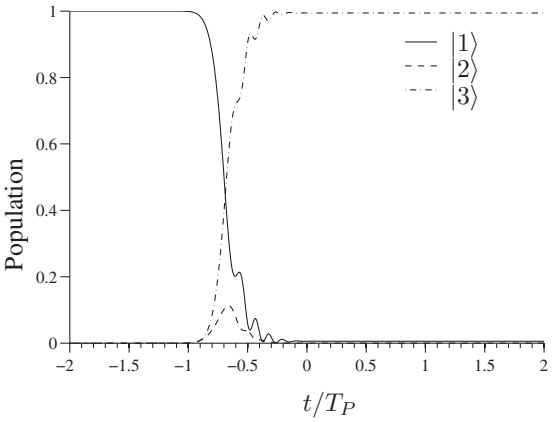

FIG. 2. The evolution of the population in the three-state-system (state $|1\rangle$ solid line, $|2\rangle$ dashed line and $|3\rangle$ dash-dotted line) where the pulses used were the original Gaussians with the following parameters: $\Delta_P=30/T_P$, $\Delta_S=45/T_P$, $S_0=200/T_P$, $\Omega_0=50/T_P$, $T_S=T_P$, $T_{St}=2T_P$, $\tau_p=-T_P$, and $\tau_s=-2T_P$. There was no decay out of state $|2\rangle$, $(\Gamma=0)$.

tion with no decay, and using pulse parameters out of [13] is shown in Fig. 2. For a more detailed explanation of three-state SCRAP please refer to Sec. III in Rangelov *et al.* [13].

III. OPTIMIZATION THROUGH OPTIMAL CONTROL

The above-mentioned SCRAP process has the advantage that it can tolerate large two-photon detunings, but unlike STIRAP it suffers from decay out of state $|2\rangle$. In this section we will use an optimization technique, based on the gradient ascent pulse engineering (GRAPE) algorithm by Khaneja *et al.* [14], to optimise the transfer fidelity for a set of detunings. The state of the three-level system is characterized by the density operator $\rho(t)$ with the Liouville-von Neuman equation of motion

$$\dot{\rho}(t) = -i\left[\left(H_0 + \sum_{k=1}^{m} u_k(t)H_k\right), \rho(t)\right]. \tag{12}$$

Where H_0 is the free evolution Hamiltonian (containing all the terms not dependant on the control fields, e.g., the decay $-i\Gamma$) and the H_k are the Hamiltonians corresponding to the m control fields (the Stokes, pump, and Stark fields). $u(t)=(u_1(t),u_2(t),\ldots,u_m(t))$ is the vector of control amplitudes. We discretized the transfer time T into N steps of length $\Delta t=T/N$, and assume that the amplitude for each control field is constant during each time step. Instead of optimizing these amplitudes directly for each time interval, as described in [14], we define each control field amplitude in terms of q Gaussians,

$$u_k(j) = \sum_{n=1}^{q} h_{n,k} \exp[-(j\Delta t - \tau_{n,k})^2/\sigma_{n,k}^2], \tag{13}$$

that sum to create the pulse for the specific control field, and optimize the parameters of these Gaussians. The aim is to find the parameters $(h_{n,k},\tau_{n,k},\sigma_{n,k})$ that will, given the initial density operator $\rho(0)=\rho_0$, maximize the overlap of the density operator after a time T, $\rho(T)$, with a target density operator C. The overlap is measured by the standard inner product, thus the performance index Φ_0 is given by

$$\Phi_0 = \langle C|\rho(t)\rangle. \tag{14}$$

During each time step j the evolution of the system is given by the propagator

$$U_j = \exp\left[-i\Delta t\left(H_0 + \sum_{k=1}^{m} u_k(j)H_k\right)\right]. \tag{15}$$

The performance index can then be written as

$$\Phi_0 = \langle \underbrace{U_{j+1}^{\dagger}\ldots U_N^{\dagger} C U_N \ldots U_{j+1}}_{\lambda_j} \mid \underbrace{U_j \ldots U_1 \rho_0 U_1^{\dagger}\ldots U_j^{\dagger}}_{\rho_j}\rangle. \tag{16}$$

From [14] we have that

$$\frac{\delta\Phi_0}{\delta u_k(j)} = -\langle\lambda_j|i\Delta t[H_k,\rho_j]\rangle, \tag{17}$$

but we are interested in the gradient with regard to $h_{n,k}$, $\tau_{n,k}$, and $\sigma_{n,k}$:

$$\frac{\delta\Phi_0}{\delta h_{n,k}} = \sum_{j=1}^{N}\left[\frac{\delta\Phi_0}{\delta u_k(j)}\frac{\delta u_k(j)}{\delta h_{n,k}}\right] = \sum_{j=1}^{N} -\langle\lambda_j|i\Delta t[H_k,\rho_j]\rangle \exp[-(j\Delta t - \tau_{n,k})^2/\sigma_{n,k}^2], \tag{18}$$

and similarly

$$\frac{\delta\Phi_0}{\delta\tau_{n,k}} = \sum_{j=1}^{N} -\langle\lambda_j|i\Delta t[H_k,\rho_j]\rangle \frac{2(j\Delta t - \tau_{n,k})}{\sigma_{n,k}^2} h_{n,k} \times \exp[-(j\Delta t - \tau_{n,k})^2/\sigma_{n,k}^2], \tag{19}$$

$$\frac{\delta\Phi_0}{\delta\sigma_{n,k}} = \sum_{j=1}^{N} -\langle\lambda_j|i\Delta t[H_k,\rho_j]\rangle \frac{2(j\Delta t - \tau_{n,k})^2}{\sigma_{n,k}^3} h_{n,k} \times \exp[-(j\Delta t - \tau_{n,k})^2/\sigma_{n,k}^2]. \tag{20}$$

The performance Φ_0 increases if we choose

$$h_{n,k} \to h_{n,k} + \epsilon\frac{\delta\Phi_0}{\delta h_{n,k}}, \tag{21}$$

with ϵ a small step size, and similarly for $\tau_{n,k}$ and $\sigma_{n,k}$.

We made use of a Matlab routine "minFuncBC," written by Mark Schmidt [18] to perform the final optimization step Eq. (21). It makes use of a quasi-Newton method, the Broyden-Fletcher-Goldfarb-Shanno (BFGS) method, and accepted as input Φ_0 and the vector of derivatives with respect to the optimizing parameters, $[\frac{\delta\Phi_0}{\delta h_{n,k}}, \frac{\delta\Phi_0}{\delta\tau_{n,k}}, \frac{\delta\Phi_0}{\delta\sigma_{n,k}}]$.

IV. RESULTS

In order to optimize the pulses for as large a detuning space as possible a number of points in the detuning space

TABLE I. The parameters for each of the nine Gaussians that constitute each of the pulses. The amplitudes of the Gaussians for a given pulse were all equal: $h_{n,P}=h_{n,S}=0.23\Omega_0$ and $h_{n,St}=0.23S_0$.

n	1	2	3	4	5
$\tau_{n,k}$	τ_k	$\tau_k-0.15T_k$	$\tau_k+0.15T_k$	$\tau_k-0.4T_k$	$\tau_k+0.4T_k$
$\sigma_{n,k}$	$\sqrt{0.2}T_k$	$\sqrt{0.2}T_k$	$\sqrt{0.2}T_k$	$\sqrt{0.25}T_k$	$\sqrt{0.25}T_k$
n		6	7	8	9
$\tau_{n,k}$		$\tau_k-0.55T_k$	$\tau_k+0.55T_k$	τ_k-T_k	τ_k+T_k
$\sigma_{n,k}$		$\sqrt{0.2}T_k$	$\sqrt{0.2}T_k$	$\sqrt{0.32}T_k$	$\sqrt{0.32}T_k$

was used. An initial single point in the detuning space was chosen by searching for the detuning point with optimized pulses that performed the best over the whole chosen detuning space. This entailed calculating the fidelity, using Eq. (14), for each point in the detuning space, and then taking the average. Once the first point was found a second point would be chosen by searching for the second point that, together with the first, would result in the best optimized pulses. This process would be repeated until no additional points result in better pulses. The total performance function used for evaluating the efficiency of the pulses during the optimization on a number d of detunings was taken as the average of the performance functions Eq. (14) for each of the d detuning points,

$$\Phi = \frac{1}{d}\sum_{x=1}^{d} \Phi_0(\Delta_P^x, \Delta_S^x). \tag{22}$$

The gradients for the optimizing parameters were the averages of the gradients for each of the d detuning points,

$$\frac{\delta\Phi}{\delta h_{n,k}} = \frac{1}{d}\sum_{x=1}^{d} \frac{\delta\Phi_0(\Delta_P^x, \Delta_S^x)}{\delta h_{n,k}}, \tag{23}$$

and similarly for $\tau_{n,k}$ and $\sigma_{n,k}$.

For the initial pulses used in our optimal control routine we used 9 gaussians of equal amplitude to approximate each of the original pulse shapes Eqs. (2)–(4). That is, in Eq. (13), $q=9$ and $k\in\{P,S,St\}$ (the probe, Stokes, and Stark fields). The parameters of these gaussians are given in Table I. The original pulses (solid lines in Fig. 3) had the following parameters: $S_0=200/T_P$, $\Omega_0=50/T_P$, $T_S=T_P$, $T_{St}=2T_P$, $\tau_P=-T_P$, $\tau_S=-2T_P$, and $\tau_{St}=0$.

It is always possible to increase the success of STIRAP and SCRAP by increasing the maximum Rabi frequency. However in SCRAP diabatic evolution is required after the Stark pulse peak, thus placing an upper limit on the maximum Rabi frequency, see Eq. (26) in [13]. Furthermore in every experiment there will be physical limits to the maximum Rabi frequency achievable. Once this limit is reached we can then go further to control the specific pulse shapes for both STIRAP and SCRAP to maximize the transfer. To thus provide a fair basis for comparison between STIRAP, SCRAP and the optimized SCRAP we fix identical maximum Rabi frequencies and adjust the pulse shapes. The maximum of the optimized pulses was constrained to that of the original pulses ($S_0=200/T_P$, $\Omega_0=50/T_P$). Furthermore the optimization was constrained to prevent the optimized pulses from becoming too narrow by setting the lower bound on the width of the pulses to 50% of the original pulse width. The optimized pulses are shown as the dashed lines in Fig. 3.

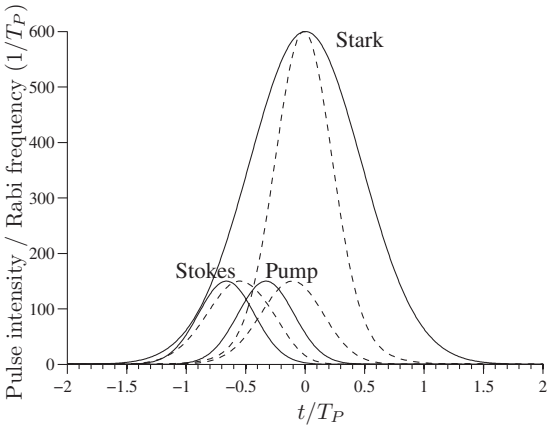

FIG. 3. The original Gaussian pulses (solid lines) with $S_0=200/T_P$, $\Omega_0=50/T_P$, $T_S=T_P$, $T_{St}=2T_P$, $\tau_p=-T_P$, and $\tau_s=-2T_P$. The dashed lines are the pulses optimized for the detunings indicated in Fig. 5 by the white dots.

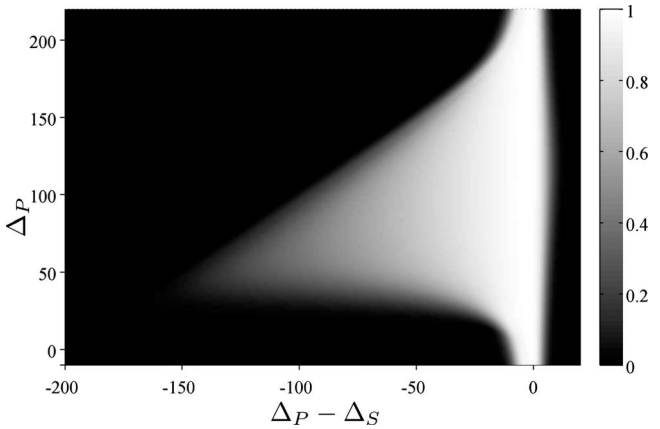

FIG. 4. The fidelity for a range of detunings, using the original Gaussian pulses for SCRAP (shown as the solid lines in Fig. 3), with $S_0=200/T_P$, $\Omega_0=50/T_P$, $T_S=T_P$, $T_{St}=2T_P$, $\tau_p=-T_P$, and $\tau_s=-2T_P$. The decay out of state $|2\rangle$ was $\Gamma=1/T_P$.

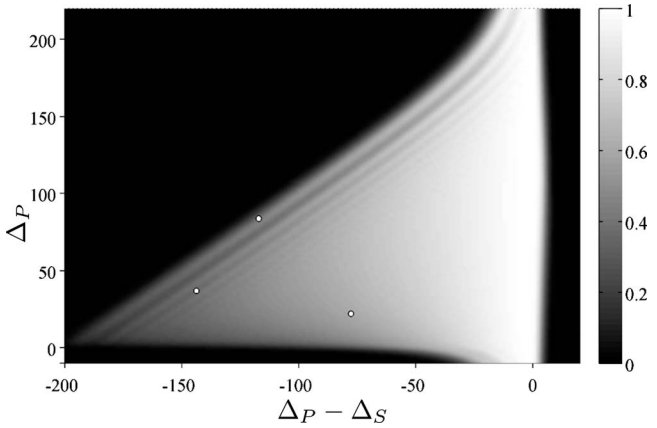

FIG. 5. The fidelity for a range of detunings, using SCRAP pulses optimized for the detunings indicated (white circles). Optimized pulses shown as the dashed lines in Fig. 3. The decay out of state $|2\rangle$ was $\Gamma = 1/T_p$.

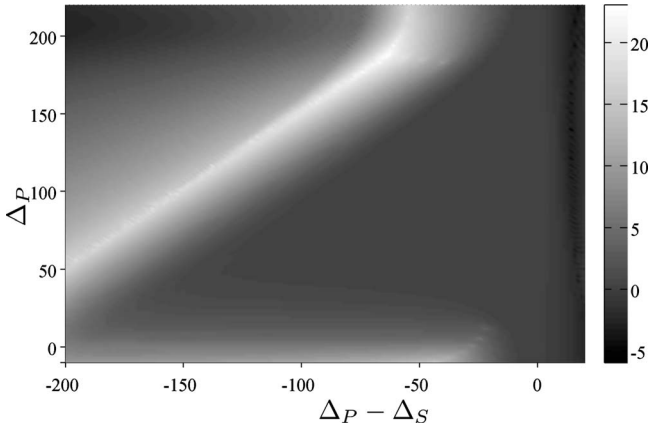

FIG. 6. The $\log_{10}$ of the percentage increase in fidelity between standard SCRAP (Fig. 4) and optimized SCRAP (Fig. 5) for each point in the detuning space.

The optimized pulses were then used to evaluate the fidelity of the population transfer from state $|1\rangle$ to state $|3\rangle$ for a range of detunings, keeping in mind that the chosen pulse ordering restricts the choice of detunings Eq. (10). As can be seen from Figs. 4 and 5 the total "area" of detunings where population transfer is at all possible (the parts that are not black) is greatly increased when using the optimized pulses. The efficiency of the pulses can be gauged in a number of ways:

(1) Measuring the normalized "area" in detuning space where the pulses result in a population transfer fidelity greater than 0.8. For the original SCRAP pulses $A^{ori}_{>0.8}=0.131$, while for the optimized pulses $A^{opt}_{>0.8}=0.178$ was obtained, an increase of 35.5%.

(2) Measuring the average fidelity over the whole detuning space, i.e., the sum of the fidelities for each point, divided by the number of points. For the original SCRAP pulses $F^{ori}_{av}=0.219$, while for the optimized pulses $F^{opt}_{av}=0.321$, an increase of 46.6%.

(3) In Fig. 6 a plot of the percentage increase for each point in the detuning space is presented. The $\log_{10}$ of the percentage increase is used since some points had an initial fidelity of virtually zero and ended with a percentage increase of $\approx 10^{23}\%$.

V. CONCLUSIONS

It is clear that Stark-shift chirped rapid adiabatic passage (SCRAP) is a useful process to employ when trying to overcome inhomogeneous broadening of energy levels in a system undergoing state transfer. We have shown that the standard SCRAP pulses can be optimized so that a larger inhomogeneous broadening can be compensated for and so that the overall fidelity of state transfer for a range of detunings will be increased. Future work will aim to translate SCRAP into the quantum domain where the pump pulse is replaced by a quantum probe field carrying quantum information that is to be stored in the spin coherence of the atomic system.

ACKNOWLEDGMENTS

J.-H.S. received financial support from Macquarie University. We would also like to acknowledge our funding sources: European Commission FP6 IST and FET QIPC project QAP Contract No. 015848, DEST ISL Grant No.CG090188 (S.R. and J.T.).

[1] S. E. Harris, Phys. Today **50** (7), 36 (1997).
[2] L. V. Hau, S. E. Harris, Z. Dutton, and C. H. Behroozi, Nature (London) **397**, 594 (1999).
[3] D. F. Phillips, A. Fleischhauer, A. Mair, R. L. Walsworth, and M. D. Lukin, Phys. Rev. Lett. **86**, 783 (2001).
[4] M. Fleischhauer and M. D. Lukin, Phys. Rev. A **65**, 022314 (2002).
[5] M. D. Lukin, Rev. Mod. Phys. **75**, 457 (2003).
[6] K. Bergmann, H. Theuer, and B. W. Shore, Rev. Mod. Phys. **70**, 1003 (1998).
[7] N. V. Vitanov, T. Halfmann, B. W. Shore, and K. Bergmann, Annu. Rev. Phys. Chem. **52**, 763 (2001).
[8] J.-H. Wu, G. C. La Rocca, and M. Artoni, Phys. Rev. B **77**, 113106 (2008).
[9] A. V. Turukhin, V. S. Sudarshanam, M. S. Shahriar, J. A. Musser, B. S. Ham, and P. R. Hemmer, Phys. Rev. Lett. **88**, 023602 (2001).
[10] J. J. Longdell, E. Fraval, M. J. Sellars, and N. B. Manson, Phys. Rev. Lett. **95**, 063601 (2005).
[11] C. Wei and N. B. Manson, J. Opt. B Quantum Semiclassical Opt. **1**, 464 (1999).
[12] P. R. Hemmer, A. V. Turukhin, M. S. Shahriar, and J. A. Musser, Opt. Lett. **26**, 361 (2001).
[13] A. A. Rangelov, N. V. Vitanov, L. P. Yatsenko, B. W. Shore, T. Halfmann, and K. Bergmann, Phys. Rev. A **72**, 053403 (2005).
[14] N. Khaneja, T. Reiss, C. Kehlet, T. Schulte-Herbrüggen, and S.

J. Glaser, J. Magn. Reson. **172**, 296 (2005).
[15] L. P. Yatsenko, B. W. Shore, T. Halfmann, K. Bergmann, and A. Vardi, Phys. Rev. A **60**, R4237 (1999).
[16] T. Rickes, L. P. Yatsenko, S. Steuerwald, T. Halfmann, B. W. Shore, N. V. Vitanov, and K. Bergmann, J. Chem. Phys. **113**, 534 (2000).
[17] J. Wrachtrup and F. Jelezko, J. Phys.: Condens. Matter **18**, S807 (2006).
[18] http://www.cs.ubc.ca/~schmidtm/Software/minFunc.html.